Geochemical Journal, Vol. 41, pp. 341 to 357, 2007

Petrogenesis of Karamaili alkaline A-type granites from East Junggar, Xinjiang (NW China) and their relationship with tin mineralization

YUPING SU,[1,2] HONGFENG TANG,[1]* PAUL J. SYLVESTER,[3] CONGQIANG LIU,[1] WENJUN QU,[4] GUANGSHUN HOU[1,2] and FENG CONG[1,2]

[1]Laboratory for Study of the Earth's Interior and Geofluids, Institute of Geochemistry, Chinese Academy of Sciences, Guiyang 550002, China
[2]Graduate School of Chinese Academy of Sciences, Beijing 100049, China
[3]Department of Earth Sciences, Memorial University of Newfoundland, St. John's, Newfoundland A1B 3X5, Canada
[4]National Research Center of Geoanalysis, Chinese Academy of Geological Sciences, Beijing 100037, China

(*Received October 23, 2006; Accepted July 18, 2007*)

Several types of granites including alkaline granites and alkali feldspar granites are distributed in the Karamaili tectonic belt of East Junggar, Xinjiang, China. Some medium-small tin deposits are located within or near the contact zones of the granitic intrusions. The alkaline granites share all the features commonly observed in peralkaline A-type granites. They contain alkalic mafic minerals such as riebeckite and aegirine; have high contents of SiO_2, alkalis, Rb, Th, Zr, Hf, REE (except Eu), and high ratios of FeO*/MgO and Ga/Al; and show strong depletions in Ba, Sr, Eu in the spidergrams. Laser ablation-ICPMS U–Pb zircon geochronology indicates a crystallization age of *ca*. 305 Ma for the granites; TIMS analyses of the granites found high $\varepsilon_{Nd}(T)$ values of +5.9 to +6.5. Considering their geochemical features, alkaline granites most likely formed by fractional crystallization of granodioritic magmas, which were probably produced by partial melting of lower crustal basaltic to andesitic rocks formed from oceanic crustal materials that were deeply buried during late Paleozoic subduction and accretion. Six molybdenite samples from the Sareshike tin deposit in East Junggar yielded an isochron age of 307 ± 11 Ma (2σ) and a weighted mean model age of 306.5 ± 3.4 Ma, consistent with zircon U–Pb ages of the alkaline granites. Low Re contents (0.323–0.961 ppm) in the molybdenite suggest that they originated from crustal sources related to the alkaline granites. Considering their identical ages, close spatial distribution, and similar sources, we argue that the A-type granites have a genetic relationship with the tin mineralization, and that the same association may be important elsewhere.

Keywords: alkaline granites, tin deposits, zircon U–Pb dating, Re–Os isochron, petrogenesis, East Junggar

INTRODUCTION

The origin and significance of A-type granite is currently one of the most debated topics in petrology and geochemistry. Unlike I- (igneous) and S- (sedimentary) type granites, the original definition of A-type granites did not imply a specific source, but instead emphasized what was thought to be their "anorogenic" tectonic setting and relatively alkaline and anhydrous magmatic character (Chappell and White, 1974; Loiselle and Wones, 1979). However, more recent studies have shown that A-type granites can contain water up to several weight percent (Clemens *et al*., 1986; Klimm *et al*., 2003), can be metaluminous or even peraluminous (Collins *et al*., 1982; Rajesh, 2000; Vernikovsky *et al*., 2003), and occur in a variety of tectonic settings such as post-collision (Sylvester, 1989; Nardi and Bonin, 1991). Thus the scope of the term, A-type granites, has been broadened to some extent. Consequently, many scholars cast doubt on the meaning of the term "A-type" (Creaser *et al*., 1991; Frost *et al*., 2001). Nonetheless, the distinctive petrological, mineralogical and geochemical features and great economic value of granites that have been described as "A-type" continue to make them the focus of ongoing interest (Collins *et al*., 1982; Whalen *et al*., 1987; Eby, 1990, 1992; Landenberger and Collins, 1996).

Several petrogenetic models for A-type granites have been proposed, including: (1) extensive fractional crystallization from mantle-derived mafic magmas (Turner *et al*., 1992; Han *et al*., 1997); (2) interaction of mantle-derived magmas and overlying crustal rocks (Kerr and Fryer, 1993); (3) anatexis of middle or lower crustal source rocks (Collins *et al*., 1982; Creaser *et al*., 1991); and (4) metasomatism of granitic magmas (Taylor *et al*., 1981). Considering their widespread distribution in space and time from the Archean to the Cenozoic (Kerr and

*Corresponding author (e-mail: tanghongfeng@vip.gyig.ac.cn)

Fryer, 1993; Sylvester, 1994; Wu *et al*., 2002), the variety of tectonic settings in which they formed, the complexity of associated rocks (Collins *et al*., 1982; Turner *et al*., 1992; Rajesh, 2000; Frost *et al*., 2002), and perhaps most importantly, the large geochemical differences in major and trace element and Sr–Nd isotopic compositions between different A-type granitic intrusions, it appears that these magmas can be generated by a variety of processes and from various sources. Thus, no general petrogenetic model can be used to explain all A-type granites. Also, while numerous papers about A-type granites have discussed their petrogenesis and tectonic setting, the relationship between A-type granites and association mineralization is not well understood. This paper examines the petrogenesis of A-type granites from northwestern China and their relationship with associated tin mineralization.

The A-type granites of this study are from Northern Xinjiang, which contains large amounts of mineral resources, and is a part of the gigantic Central Asian Orogenic Belt. Its special tectonic significance and great economic potential have drawn geologists from China and other countries to the area. On each side of Junggar Basin in Northern Xinjiang, immense volume of A-type granites with high, positive $\varepsilon_{Nd}(T)$ values were emplaced. These rocks may be crucial for us to understand important issues such as the nature of the basement beneath the Junggar Basin, Phanerozoic crustal growth models, and deep seated geologic processes in Northern Xinjiang. Although Chen and Jahn (2004), Chen and Arakawa (2005) and Han *et al*. (1997) have discussed A-type granites from West Junggar and Ulungur River area, East Junggar, few studies have been performed on Karamaili A-type granites from East Junggar. The Karamaili region is an important tin metallogenic belt, in which some medium-small tin deposits are located within or near the contact zones of granitic intrusions, and these deposits have been thought to be closely related to the origin of the granitic magmatism (Bi *et al*., 1993; Liu *et al*., 1997; Yu *et al*., 1998). However, there is little direct information on the age of mineralization and the source of ore-forming materials.

In this paper, we present new zircon U–Pb ages and geochemical and Nd isotopic compositions for the alkaline A-type granites distributed to the north of the Karamaili tectonic belt, and report Re–Os isotopic ages of molybdenite samples from the Sareshike tin deposit. The petrogenesis of the alkaline granites and their relationship with the tin deposits are discussed on the basis of the available geochemical and isotopic data.

Geological Setting

The East Junggar region is located geographically at the northeastern margin of Junggar Basin, Xinjiang, and tectonically at the juncture of Siberian and Kazakhstan–Junggar palaeoplates. Three NW-SE trending A-type granite belts are distributed in this region, from north to south along the Irtysh–Mayinebo, Ulungur and Karamaili faults respectively (Xin *et al*., 1995). Han *et al*. (1997) found that the alkaline A-type granites along the Ulungur fault were emplaced at about 300 Ma with $\varepsilon_{Nd}(T)$ values ranging from +5.1 to +6.7, and proposed that they formed through extensive fractional crystallization of mantle-derived mafic magmas.

Parallel to the A-type granite belts, two ophiolite belts, Aermantai and Karamaili, occur sporadically along deep faults. The Karamaili ophiolite has been considered to be a remnant of a small oceanic crust (Li *et al*., 1990; Li, 1995), but its age is still controversial. Shu and Wang (2003) and Tang *et al*. (2007) suggested a middle-late Devonian age. Plagiogranites within Karamaili ophiolite suite have a SHRIMP U–Pb zircon age of 373 ± 10 Ma, and their $\varepsilon_{Nd}(T)$ values are about +9.4, which is suggestive of derivation from depleted mantle (Tang *et al*., 2007). Based on the study of the ophiolites, tectonic evolution of the East Junggar area is thought to have occurred in four main stages: continental crust stretching (Precambrian), oceanic basin formation (Ordovician–Silurian), oceanic basin subduction (Devonian–Carboniferous), and post-orogenic extension (late Carboniferous–early Permian) (Wang *et al*., 2003).

The stratigraphic sequence outcropping in the study area is mainly composed of Devonian to Carboniferous tuffaceous siltstones and volcanoclastics (Fig. 1). A few Silurian rocks are scattered to the south of the Karamaili tectonic belt. Granitic magmatism occurs extensively in this area, which produced many types of rocks including I-type monzogranites and granodiorites, as well as A-type hornblende granites, biotite granites and alkaline granites (Fig. 1). All of these granitic intrusions are developed as hypabyssal, shallow-hypabyssal apophyses or small stocks. A-type biotite granites crop out widely, but the I-type granodiorites are restricted to a small area. For a long time, biotite granites and hornblende granites which are rich in alkalis but do not contain alkali mafic minerals were thought to be of S-type character and origin (Bi *et al*., 1993; Yu *et al*., 1998); however, the recent study conducted by Su *et al*. (2006) concluded that they are actually typical aluminous A-type granites.

It is notable that many medium-small tin deposits (such as Sareshike and Beilekuduke) are located within or near the contact zones of granitic intrusions; these deposits are being mined at a small scale. In accordance with the mineral association and their occurrence, the ores can be divided into three types including cassiterite-quartz vein, greisen, and stanniferous altered granite types. Granite alteration including greisenization, albitization, and po-

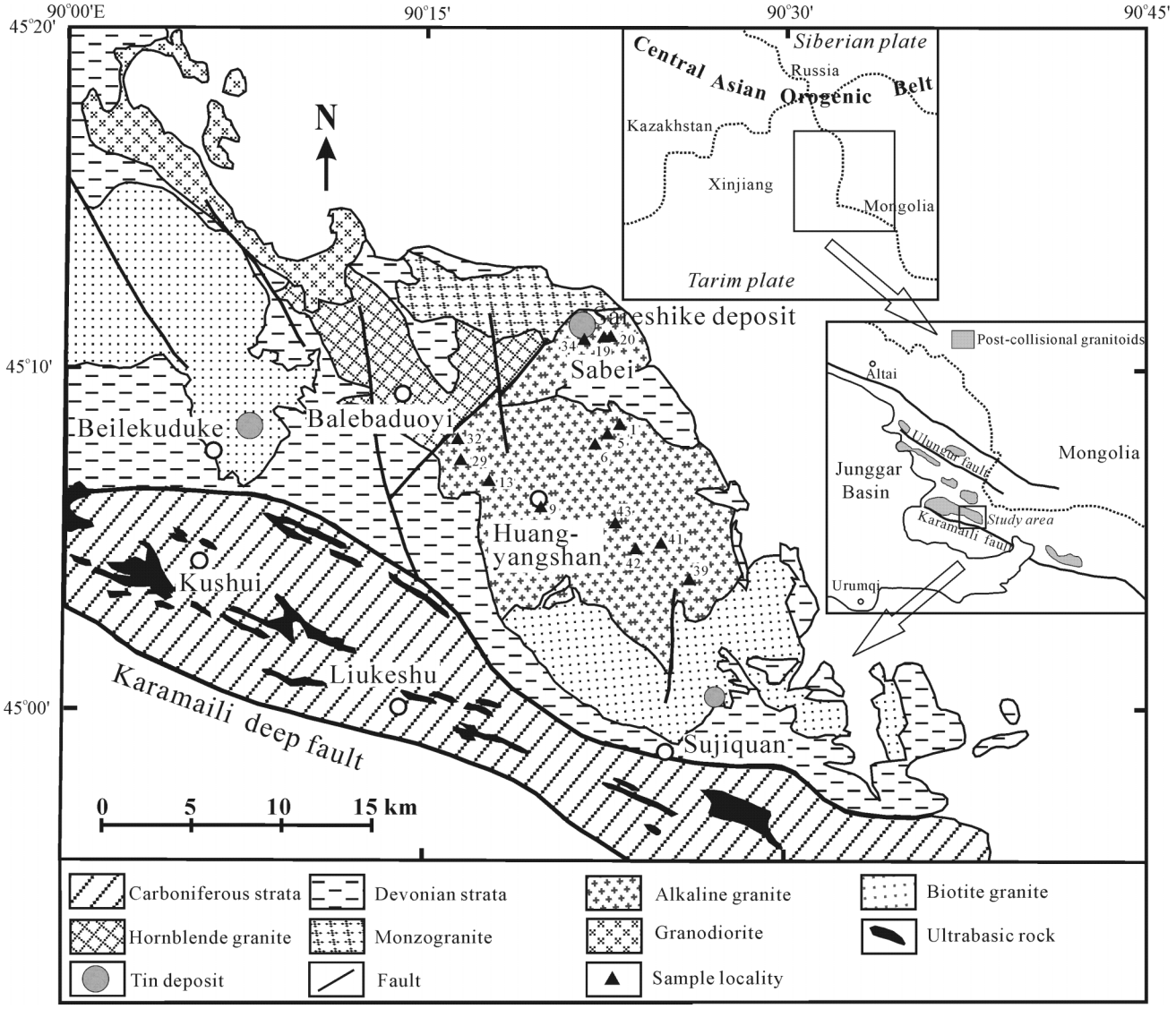

Fig. 1. Geological sketch map showing the distribution of Karamaili granitoids in East Junggar. The relationship of the study area to the Central Asian Orogenic Belt (CAOB) is shown in the upper right inset, dashed line represents national boundary. The middle right inset is a sketch map of the East Junggar foldbelt (modified from Chen and Jahn, 2004). Sample sites are indicated with numbers corresponding to sample numbers in Table 3, with the exclusion of the "HY" prefix. Three samples (HY19, HY20, HY34) are from Sabei pluton, the others from Huangyangshan pluton.

tassic alteration is closely associated with the mineralization.

PETROLOGICAL DESCRIPTION

The alkaline granites are light gray to red in colour, and massive with a fine- to coarse-grained granitic texture. Miarolitic cavities with diameters of 0.1 to 0.2 centimeter are sometimes observed. These rocks are mainly composed of alkali feldspar and quartz, with small amounts of plagioclase and mafic minerals such as amphibole. Alkali feldspar is dominantly perthite, and plagioclase is mostly albite plus small abundances of oligoclase. Quartz-alkali feldspar intergrowths and micrographic textures are common. Mafic minerals consist of amphibole and minor aegirine and biotite, which mainly form irregular crystals interstitial to alkali feldspar and quartz. Among them, amphibole is riebeckite and arfvedsonite that occurs as prismatic, subhedral to euhedral grains; biotite has Fe-rich and Mg-poor compositions that are siderophyllite (Liu *et al*., 1996) and forms subhedral to euhedral flakes. Aegirine occurs as short

prismatic, subhedral to anhedral grains found as cores in amphibole; relics of aegirine partly reacted to riebeckite are often present. Accessory minerals include zircon and Fe-oxide. Notably, both fine-grained mafic enclaves and leucogranitic enclaves are common in the alkaline granites.

The ores in this study were collected from the Sareshike tin deposit, which is mainly of the cassiterite-quartz vein type. The ore minerals include cassiterite, with minor magnetite, molybdenite, and chalcopyrite. The gangue minerals are dominated by quartz, accompanied by feldspar, riebeckite and muscovite. It is notable that molybdenite was found for the first time in these deposits. Six molybdenite samples were selected from one tunnel. They occur as blocky or disseminated crystals embedded in other minerals.

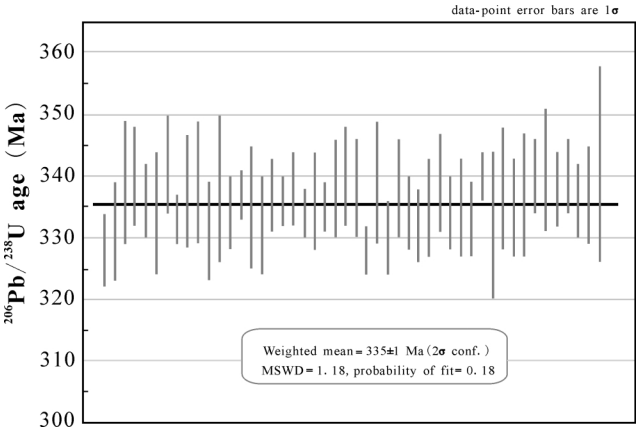

Fig. 2. LA-ICPMS $^{206}Pb/^{238}U$ ages for replicate analyses (n = 48) of the Plešovice zircon. The weighted mean of all the LA-ICPMS ages is 335 ± 1 Ma (2SD), which compares well with the isotope dilution-TIMS $^{206}Pb/^{238}U$ age of 336.9 ± 0.2 Ma (2SD) determined by Sláma et al. (in review).

Analytical Methods

Major-element concentrations of whole rock samples were analysed by wet chemical method at Institute of Geochemistry, Chinese Academy of Sciences (CAS). Trace-element concentrations were obtained by inductively coupled plasma-mass spectrometry (ICP-MS) at Guangzhou institute of Geochemistry, CAS. Sm–Nd isotopic analyses were conducted on a multicollector MAT-262 Thermal Ionization Mass Spectrometer (TIMS) in static mode at Memorial University of Newfoundland (MUN), Canada. Approximately 0.1 g of whole-rock powder was dissolved using a mixture of HNO_3–HF acids, and Nd was separated using standard ion exchange chemical techniques. Repeated TIMS measurements made during this study gave a $^{143}Nd/^{144}Nd$ ratio of 0.511885 ± 15 (2σ, $n = 25$) for the La Jolla Nd standard. All of the measured $^{143}Nd/^{144}Nd$ ratios were normalized to $^{146}Nd/^{144}Nd = 0.7219$ to correct for instrumental mass fractionation, and the reported Nd isotopic ratios have been adjusted relative to the recommended value (0.511860) for the La Jolla Nd standard.

U–Pb zircon analyses for granites were measured by laser ablation (LA)-ICPMS at MUN. All zircon grains were separated by routine approaches employing heavy liquids, purified by handpicking carefully under a binocular microscope, and mounted in epoxy. Cathodoluminescence images (CL) were made prior to isotopic measurements in order to facilitate locating sample sites in petrographic mounts and study the internal structure of the grains. U–Pb isotopic analyses were carried out on a HP 4500 ICP-MS linked to a New Wave Research UP-213 Nd:YAG laser ablation system ($\lambda = 213$ nm). A laser frequency of 10 Hz and a spot size of 40 μm were used for ablation. The ablated material was continuously transported in helium gas (1.2 l/min) from the ablation cell to ICP-MS for isotopic measurement, being mixed with argon just prior to the torch. During the analytical sessions, in-house standard 02123, a natural zircon with U–Pb isotopic age of 295 Ma, was used to correct for mass bias and U–Pb fractionation. Mass 204 was monitored to ensure there were no significant amounts of common Pb present in any particular analyses. Raw data were processed using the software program, LAMTRACE (Jackson *et al*., 1996). Weighted mean ages and concordia plots were determined using the program of Isoplot/Ex (Ludwig, 1999). The Plešovice zircon reference standard (Sláma *et al*., in review) was analysed as an unknown to evaluate the accuracy of the LA-ICPMS measured ages. The weighted mean of the $^{206}Pb/^{238}U$ ages determined for the Plešovice zircon in this study (Fig. 2) is consistent with the accepted age, 336.9 ± 0.2 Ma (2SD), determined previously by isotope dilution-TIMS (Sláma *et al*., in review).

Molybdenite Re–Os isotopic analyses were performed in the National Research Center of Geoanalysis, Chinese Academy of Geosciences. All analyzed molybdenite grains were crushed and dipped in hydrofluoric acid (in order to dissolve quartz associated with molybdenite) and then purified by handpicking carefully under a binocular microscope. The purity of the mineral separates exceeds 98%. The details of the chemical procedure have been described by Du *et al*. (1994), Shirey and Walker (1995), Markey *et al*. (1998), Stein *et al*. (2001) and Qu and Du (2003). In order to determine the Re and Os contents in molybdenite accurately, a mixed ^{190}Os and ^{185}Re spike solution was added to the bottom part of a Carius tube in which the weighed sample was loaded through a long thin-neck funnel. Separation of Os was achieved by distillation firstly, and then separation of Re by extraction. A

Table 1. Zircon LA-ICPMS U–Pb analysis for the alkaline granites from East Junggar

Sample	Spot number	Atomic ratios						Ages (Ma)			
		$^{206}Pb/^{238}U$	$\pm1\sigma$	$^{207}Pb/^{235}U$	$\pm1\sigma$	$^{207}Pb/^{206}Pb$	$\pm1\sigma$	$^{206}Pb/^{238}U$	$\pm1\sigma$	$^{207}Pb/^{235}U$	$\pm1\sigma$
HY13	1.1	0.0478	0.0002	0.3566	0.0018	0.0541	0.0004	301	1	310	2
	2.1	0.0493	0.0003	0.3492	0.0025	0.0514	0.0005	310	2	304	2
	3.1	0.0474	0.0005	0.3484	0.0036	0.0533	0.0002	299	3	303	2
	4.1	0.0483	0.0006	0.3527	0.0056	0.0529	0.0012	304	3	307	4
	5.1	0.0486	0.0006	0.3532	0.0045	0.0528	0.0009	306	4	307	3
	6.1	0.0485	0.0006	0.3464	0.0049	0.0518	0.0006	305	3	302	4
	7.1	0.0499	0.0004	0.3577	0.0045	0.0520	0.0005	314	3	311	4
	8.1	0.0483	0.0006	0.3616	0.0083	0.0542	0.0008	304	3	313	6
	9.1	0.0476	0.0005	0.3564	0.0039	0.0543	0.0003	300	3	310	3
	10.1	0.0482	0.0003	0.3572	0.0095	0.0537	0.0010	303	1	310	7
	11.1	0.0470	0.0005	0.3457	0.0049	0.0534	0.0003	296	3	301	3
	12.1	0.0481	0.0005	0.3558	0.0069	0.0537	0.0007	303	3	309	5
	13.1	0.0474	0.0004	0.3502	0.0035	0.0535	0.0005	299	2	305	3
	14.1	0.0466	0.0004	0.3403	0.0042	0.0530	0.0005	293	2	297	3
	15.1	0.0494	0.0004	0.3590	0.0030	0.0527	0.0008	311	3	311	2
	16.1	0.0481	0.0003	0.3532	0.0042	0.0533	0.0004	303	2	307	3
	17.1	0.0482	0.0003	0.3690	0.0025	0.0555	0.0004	303	2	319	2
	18.1	0.0484	0.0005	0.3509	0.0055	0.0526	0.0003	305	4	305	4
	19.1	0.0468	0.0006	0.3389	0.0099	0.0526	0.0017	295	4	296	7
	20.1	0.0479	0.0007	0.3410	0.0128	0.0516	0.0019	302	4	298	10
HY32	1.1	0.0487	0.0003	0.3570	0.0163	0.0532	0.0023	306	1	310	12
	2.1	0.0505	0.0004	0.3553	0.0084	0.0510	0.0010	318	3	309	7
	3.1	0.0514	0.0009	0.3731	0.0155	0.0526	0.0015	323	5	322	12
	4.1	0.0509	0.0004	0.3554	0.0052	0.0507	0.0009	320	2	309	4
	5.1	0.0507	0.0004	0.3737	0.0056	0.0535	0.0010	319	3	322	4
	6.1	0.0486	0.0003	0.3498	0.0029	0.0522	0.0004	306	2	305	3
	7.1	0.0487	0.0004	0.3472	0.0158	0.0517	0.0022	307	3	303	12
	8.1	0.0488	0.0011	0.3407	0.0169	0.0506	0.0017	307	6	298	13
	9.1	0.0485	0.0007	0.3426	0.0059	0.0513	0.0008	305	4	299	4
	10.1	0.0509	0.0010	0.3661	0.0136	0.0522	0.0014	320	6	317	10
	11.1	0.0486	0.0004	0.3640	0.0132	0.0543	0.0021	306	3	315	10
HY19	1.1	0.0475	0.0009	0.3601	0.0246	0.0550	0.0025	299	6	312	18
	1.2	0.0475	0.0006	0.3381	0.0038	0.0516	0.0004	299	3	296	3
	2.1	0.0495	0.0014	0.3546	0.0213	0.0519	0.0022	312	9	308	16
	3.1	0.0461	0.0008	0.3325	0.0064	0.0523	0.0005	291	5	291	4
	4.1	0.0495	0.0006	0.3582	0.0056	0.0525	0.0006	311	3	311	4
	5.1	0.0485	0.0005	0.3486	0.0048	0.0522	0.0004	305	3	304	4
	5.2	0.0486	0.0010	0.3476	0.0046	0.0519	0.0008	306	6	303	4
	6.1	0.0483	0.0006	0.3528	0.0201	0.0530	0.0029	304	3	307	15
	6.2	0.0487	0.0004	0.3488	0.0095	0.0520	0.0013	306	2	304	7
	6.3	0.0485	0.0007	0.3677	0.0210	0.0550	0.0015	305	4	318	16
	7.1	0.0481	0.0005	0.3576	0.0028	0.0539	0.0004	303	3	310	2
	8.1	0.0499	0.0006	0.3639	0.0034	0.0528	0.0006	314	3	315	2
	9.1	0.0476	0.0014	0.3264	0.0082	0.0497	0.0009	300	9	287	6
	10.1	0.0495	0.0004	0.3591	0.0036	0.0526	0.0007	312	3	312	3
	11.1	0.0479	0.0004	0.3472	0.0035	0.0525	0.0004	302	3	303	3
	11.2	0.0481	0.0004	0.3618	0.0157	0.0546	0.0016	303	3	314	12
	12.1	0.0518	0.0007	0.3719	0.0058	0.0521	0.0003	325	4	321	4
	13.1	0.0479	0.0008	0.3435	0.0028	0.0520	0.0007	302	5	300	2

Note: HY13, HY32 from Huangyangshan pluton, HY19 from Sabei pluton. All data listed were used to calculate the weighted mean ages.

TJA PQ-EXCELL ICP-MS was used for the determination of Re and Os isotopic ratios. Average blanks for the total Carius tube procedure were *ca.* 23 pg for Re and <0.1 pg for ^{187}Os. The analytical reliability was tested by duplicate analyses of molybdenite standard HLP-5 from a carbonatite vein-type molybdenum-lead deposit in the Jinduicheng-Huanglongpu area of Shaanxi Province, China. The preferred Re–Os age for HLP-5 has been given

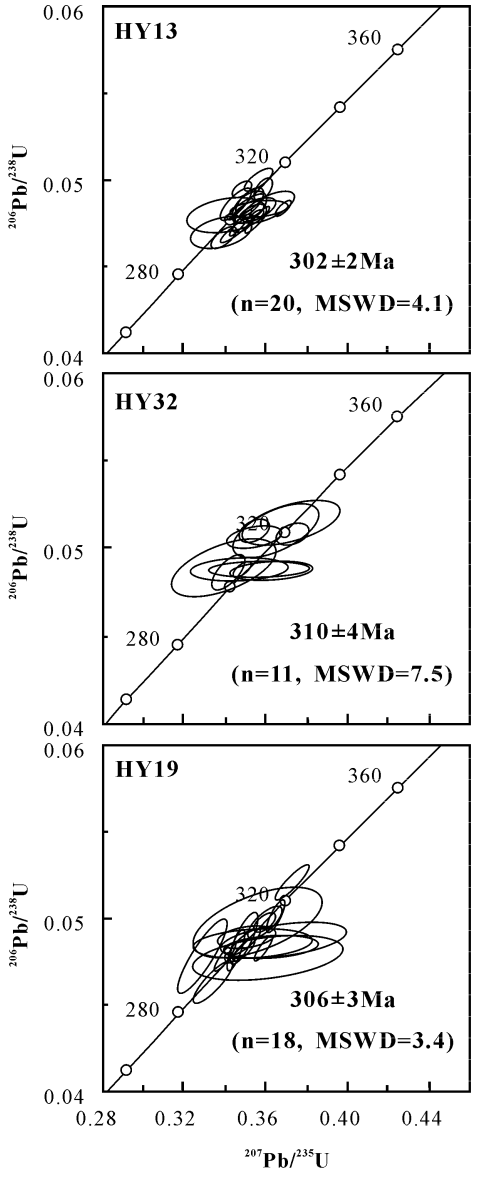

Fig. 3. Concordia age diagrams of single-grain zircon U–Pb LA-ICPMS analyses on the alkaline granites from East Junggar.

as 221.3 ± 0.3 Ma (Stein *et al*., 1997), and two measurements of HLP-5 made in this study gave ages of 218.3 ± 2.6 Ma and 218.9 ± 2.8 Ma. The age uncertainty for each sample is about 1.3% resulting from uncertainties of the ^{187}Re decay constant, the isotopic measurements and spike calibrations.

GEOCHRONOLOGY

Ages of the alkaline granites

All the zircons selected for analysis are igneous in origin, being characterized in particular by highly transparency, euhedral form, and clear, oscillatory zonation. The U–Pb analytical results for the zircons are given in Table 1 and Fig. 3. In conventional U–Pb concordia diagrams (Fig. 3), most zircon grains plot on the concordia, and only a few points deviate slightly off it. The weighted mean $^{206}Pb/^{238}U$ ages are shown in Fig. 3 and are the preferred ages for concordant samples because uncertainties in the blank and common Pb composition has little influence on this age, whereas it can affect the $^{207}Pb/^{235}U$ and $^{207}Pb/^{206}Pb$ ages dramatically.

Three $^{206}Pb/^{238}U$ ages for the alkaline granites were obtained, two from Huangyangshan with ages of 302 ± 2 Ma (n = 20, MSWD = 4.1) and 310 ± 4 Ma (n = 11, MSWD = 7.5), the third one from Sabei with age of 306 ± 3 Ma (n = 18, MSWD = 3.4). All these results are similar to one another so their average age (*ca*. 305 Ma) can be taken as the emplacement age of the alkaline granites. Su *et al*. (2006) reported U–Pb isotopic data for the zircons from the neighboring alkali feldspar granites at Sujiquan. The $^{206}Pb/^{238}U$ age for Sujiquan body is 304 ± 2 Ma, consistent with the ages of the alkaline granites determined in this study. This consistency, plus similar $\varepsilon_{Nd}(T)$ values (discussed below), suggests that the alkaline granites and alkali feldspar granites might be the products of cogenetic magmas.

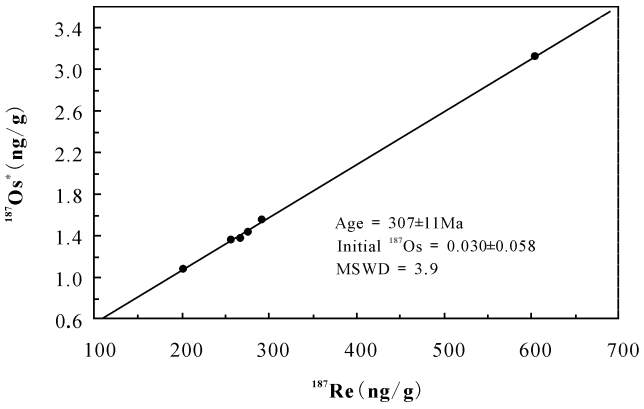

Fig. 4. Re–Os isochron plot for molybdenite samples from Sareshike tin deposit, East Junggar.

Ages of mineralization

The concentrations of Re and Os and the osmium isotopic compositions of molybdenite from the Sareshike tin deposit are presented in Table 2. In general, molybdenite (MoS_2) can incorporate Re but contain little or no Os at the time of crystallization (Mao *et al*., 1999; Stein *et al*., 2001). In practice, actual measurements indicate that molybdenite from some deposits contain minor but significant common (initial) Os (Mao *et al*., 2003; Hou *et al*., 2004) and this is the case for the molybdenite studied here (especially in sample HY38-1). Thus, initial ^{187}Os

Table 2. Re–Os isotopic data for molybdenites from Sareshike tin deposit, East Junggar

Sample No.	Sample weight (g)	Common Os (ng/g)	Re (ng/g)	^{187}Re (ng/g)	^{187}Os (ng/g)	^{187}Os* (ng/g)	Model age (Ma)
HY38-1	0.40115	0.2277 (0.0062)	323.1 (2.5)	203.1 (1.6)	1.111 (0.010)	1.069 (0.010)	306.4 (4.0)
HY38-2	0.39968	0.0240 (0.0012)	960.9 (8.2)	604.0 (5.1)	3.125 (0.023)	3.120 (0.023)	306.3 (3.7)
HY38-3	0.39987	0.0559 (0.0026)	439.4 (3.4)	276.2 (2.1)	1.448 (0.013)	1.437 (0.013)	305.1 (3.9)
HY38-4	0.40038	0.0339 (0.0015)	425.8 (3.3)	267.7 (2.1)	1.383 (0.013)	1.377 (0.013)	301.3 (4.0)
HY38-5	0.40033	0.0429 (0.0013)	409.5 (4.1)	257.4 (2.6)	1.365 (0.011)	1.357 (0.011)	308.7 (4.2)
HY38-6	0.40082	0.0734 (0.0007)	464.3 (3.9)	291.8 (2.4)	1.560 (0.013)	1.546 (0.013)	311.1 (3.9)

Note: Values in parenthesis are absolute uncertainties (2σ). Decay constant used for ^{187}Re is 1.666 × 10^{-11}/year. Our analyses indicate that common Os in molybdenite samples (especially in sample HY38-1) is present, so initial ^{187}Os values must be subtracted when calculating ^{187}Os–^{187}Re isochron age and Re–Os model ages. The corrected ^{187}Os concentrations (^{187}Os) were determined from the measured ^{187}Os values, ^{187}Os/^{188}Os ratios, and the initial Os isotopic composition.*

abundances must be subtracted before Re–Os model ages are calculated. The analytical results show that total Re and ^{187}Os concentrations of the molybdenite range from 323.1 to 960.9 ng/g and 1.111 to 3.125 ng/g respectively, and model ages for six individual analyses vary from 301.3 to 311.1 Ma, which yields a weighted mean age of 306.5 ± 3.4 Ma. When plotted in ^{187}Os* vs. ^{187}Re diagram (Fig. 4), six points define an isochron with an age of 307 ± 11 Ma (MSWD = 3.9) and initial ^{187}Os of 0.030 ± 0.058 ng/g. This value is consistent (within analytical uncertainty) with the U–Pb zircon ages (*ca*. 305 Ma) of the alkaline granites.

Liu *et al*. (1996) reported a U–Pb zircon age of 263.6 ± 3 Ma from cassiterite-quartz veins as an age of mineralization; obviously, their result is significantly younger than that of our study. The reason for this discrepancy is not clear, because Liu *et al*. (1996) presented their result without original data or a detailed explanation. Chen *et al*. (1999) obtained a mineralization age of 305 ± 25 Ma for the Ganliangzi tin deposit occurring in the same tin metallogenic belt as the Sareshike deposit, derived by Rb–Sr dating of fluid inclusions hosted by quartz grains. Their result is in good agreement with our Re–Os age, though less precise. Nevertheless, the agreement between U–Pb, Re–Os and Rb–Sr isotopic results suggests that both A-type granite magmatism and mineralization in the tin metallogenic belt in eastern Junggar probably formed about 305 Ma ago (late Carboniferous).

GEOCHEMISTRY

Major and trace elements

The major- and trace-element compositions for the alkaline granites are given in Table 3. The rocks are highly siliceous, with SiO_2 content ranging from 74.31 to 79.83 wt%. They have low abundances of Al_2O_3 (7.68–11.65 wt%), CaO (0.18–0.99 wt%), MgO (0.10–0.26 wt%), FeO* (1.70–3.15 wt%), and high contents of alkalis with $Na_2O + K_2O$ = 7.03%–8.41 wt%. All these characteristics are typical of A-type granites. MnO abundances range

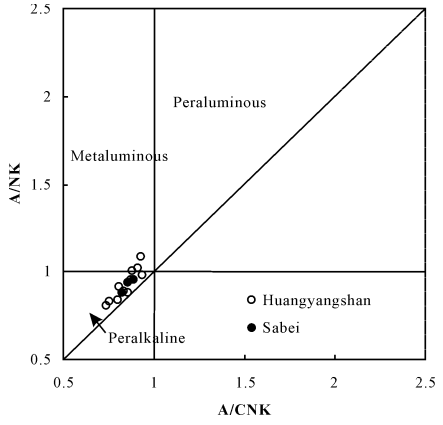

Fig. 5. A/NK vs. A/CNK plot for the alkaline granites from East Junggar. Most of the samples fall in the peralkaline field.

from 0.10% to 0.18 wt%, which is about 2–3 times higher than average A-type granites worldwide (0.06 wt%, Whalen *et al*., 1987); and their FeO*/MgO ratios range from 9.52 to 31.5, most of which are higher than those of fractionated I- and S-type granites (Whalen *et al*., 1987). In the diagram of A/NK vs. A/CNK (Fig. 5), the alkaline granites plot mainly in peralkaline field. From a CIPW calculation, most samples have normative acmite (ac) and sodium metasilicate (ns), which is consistent with their strong enrichment in alkalis and the presence of alkali mafic minerals.

In primitive-mantle normalized spidergrams (Fig. 6), the alkaline granites are enriched in some LILE (large ion lithophile elements) (Rb, Th, U, K) and HFSE (high field strength elements) (Ta, Zr, Hf), but strongly depleted in Ba, Sr, Eu, and to a lesser extent, Nb. They generally have high Sn concentrations ranging from 2.93 to 11.47 ppm, with an average value of 6.81 ppm, and pronounced positive Sn anomaly is observed in the spidergrams. Their 10000 × Ga/Al ratios are also high, ranging from 3.78 to 6.43, and clearly higher than the average values of 2.10 and 2.28 for I- and S-type granites, respectively (Whalen

Table 3. Geochemical compositions of the alkaline granites from East Junggar

Body name	Huangyangshan											Sabei		
Sample	HY1	HY5	HY6	HY9	HY13	HY29	HY32	HY39	HY41	HY42	HY43	HY19	HY20	HY34
SiO_2	74.43	78.07	75.23	76.17	76.30	77.04	79.83	75.74	74.32	74.31	74.79	76.98	77.36	76.68
TiO_2	0.50	0.47	0.45	0.47	0.56	0.46	0.43	0.53	0.40	0.50	0.48	0.48	0.53	0.53
Al_2O_3	10.66	9.00	10.33	9.87	9.28	8.74	7.68	9.80	11.65	11.39	10.59	9.74	9.00	9.27
Fe_2O_3	2.61	1.81	1.86	2.12	2.31	2.05	1.32	1.80	1.79	1.77	2.04	0.83	1.81	1.61
FeO	0.80	0.71	0.80	0.75	0.95	0.75	0.60	0.80	0.65	0.97	0.90	0.95	1.05	0.71
MnO	0.13	0.10	0.12	0.17	0.12	0.15	0.13	0.15	0.16	0.16	0.15	0.16	0.18	0.16
MgO	0.10	0.11	0.26	0.11	0.11	0.11	0.11	0.15	0.19	0.19	0.22	0.11	0.11	0.11
CaO	0.23	0.29	0.39	0.50	0.18	0.55	0.47	0.69	0.99	0.67	0.75	0.40	0.38	0.47
Na_2O	4.15	3.78	4.58	3.73	3.66	3.98	3.48	3.88	3.45	3.99	3.67	3.58	3.46	3.07
K_2O	3.78	4.16	3.83	3.90	4.12	3.70	3.55	4.06	4.70	4.29	4.21	3.98	4.13	4.48
P_2O_5	0.30	0.27	0.20	0.28	0.24	0.24	0.25	0.27	0.28	0.23	0.24	0.20	0.21	0.28
LOI	1.81	0.77	1.70	1.37	1.68	2.00	2.01	2.02	1.30	1.45	1.72	1.96	1.54	2.17
Total	99.50	99.54	99.75	99.44	99.51	99.77	99.86	99.89	99.88	99.92	99.76	99.37	99.76	99.54
A/CNK	0.94	0.80	0.83	0.88	0.86	0.76	0.74	0.81	0.93	0.92	0.88	0.89	0.83	0.86
A/NK	0.98	0.84	0.88	0.95	0.88	0.83	0.80	0.91	1.08	1.02	1.00	0.96	0.88	0.94
Sc	0.28	2.82	3.33	3.17	1.90	2.33	1.49	3.53		2.32		1.42	1.66	2.41
V		0.47	8.62	8.62	17.4	6.29	7.00	4.01		2.44		14.6	0.16	5.35
Cr	31.2	9.74	37.4	148	28.7	15.5	10.3	12.2		16.6		15.7	15.2	20.3
Co	0.78	0.84	0.70	2.15	1.08	1.01	0.75	1.08		1.71		1.07	1.12	1.27
Ni	12.8	5.26	10.2	70.9	16.4	4.89	3.80	3.57		553		4.61	4.00	5.60
Zn	225	3230	116	94.7	102	114	66.6	82.5		38.6		154	116	80.8
Ga	29.0	21.8	29.6	22.0	23.4	29.7	20.8	24.8		22.8		20.2	24.7	22.7
Rb	207	150	212	122	126	135	122	159		112		210	228	192
Sr	2.62	4.27	3.79	9.08	8.99	4.15	2.60	18.9		30.4		2.72	3.29	7.13
Y	83.7	131	38.2	52.0	58.0	38.6	34.8	88.2		47.0		68.4	107	58.4
Zr	246	947	285	541	456	257	205	268		103		543	570	330
Nb	20.2	29.6	8.14	11.2	14.8	8.25	6.65	9.93		5.47		19.3	23.1	16.1
Mo	1.22	1.56	1.60	5.90	4.00	1.31	1.22	0.83		1.34		2.64	1.11	1.69
Sn	7.78	9.58	4.86	4.50	5.62	4.42	3.31	5.18		2.93		11.5	10.9	11.2
Cs	3.68	4.29	2.71	3.38	2.65	1.68	2.14	4.89		2.68		4.34	5.11	12.2
Ba	2.86	13.3	3.44	48.8	20.5	2.53	10.4	106		120		2.97	2.90	11.6
Hf	6.86	22.3	8.54	11.8	11.6	7.10	4.81	8.79		3.51		16.6	18.1	12.0
Ta	1.46	2.68	0.75	0.97	1.20	0.56	0.41	0.71		0.55		1.70	2.09	1.37
Pb	19.0	52.2	3.86	11.6	25.4	5.40	10.2	19.1		15.7		34.1	31.7	23.3
Th	12.8	25.5	6.63	9.67	11.5	6.79	4.29	11.0		7.88		17.6	22.4	15.3
U	3.43	5.61	1.55	2.32	2.90	1.57	1.04	2.76		1.98		6.06	6.24	4.40
La	25.5	47.8	9.46	30.5	36.1	23.4	22.2	30.7		20.6		26.8	34.5	31.0
Ce	60.4	114	23.7	67.1	74.0	54.4	48.4	75.1		50.2		68.0	81.6	68.7
Pr	8.78	14.7	3.29	8.30	9.59	7.07	6.03	9.96		6.42		7.59	10.5	9.15
Nd	39.0	63.1	14.6	34.8	39.2	30.2	25.6	43.0		27.1		31.2	44.7	38.3
Sm	11.4	17.4	4.58	8.17	8.76	7.39	5.66	11.7		6.89		8.45	12.8	9.73
Eu	0.06	0.14	0.03	0.11	0.08	0.04	0.06	0.18		0.17		0.02	0.03	0.04
Gd	13.6	22.9	6.35	9.04	9.29	7.93	6.26	15.6		8.05		10.2	17.0	10.8
Tb	2.14	3.76	1.11	1.44	1.52	1.23	0.98	2.52		1.36		1.77	2.86	1.70
Dy	12.8	23.7	7.21	8.95	9.64	7.33	5.84	16.0		8.16		11.2	18.2	10.3
Ho	2.78	5.06	1.57	1.96	2.07	1.57	1.23	3.37		1.80		2.42	4.02	2.23
Er	7.93	14.4	4.81	5.70	6.24	4.76	3.53	9.13		5.04		7.02	11.6	6.54
Tm	1.21	2.08	0.75	0.87	0.93	0.75	0.51	1.26		0.74		1.06	1.71	0.99
Yb	8.10	12.7	5.51	5.91	6.28	5.55	3.38	7.79		4.43		6.91	10.9	6.88
Lu	1.25	1.77	0.86	0.92	0.92	0.96	0.52	1.11		0.64		0.97	1.54	1.04
$10000 \times Ga/Al$	5.14	4.58	5.41	4.20	4.76	6.43	5.12	4.79		3.78		3.92	5.18	4.62
Eu/Eu*	0.02	0.02	0.02	0.04	0.03	0.02	0.03	0.04		0.07		0.01	0.01	0.01

Note: A/CNK = molar ratio of $Al_2O_3/(CaO + Na_2O + K_2O)$, A/NK = molar ratio of $Al_2O_3/(Na_2O + K_2O)$. The last three samples (HY19, HY20, HY34) from Sabei pluton, the others from Huangyangshan pluton.

et al., 1987). In discrimination diagrams for granites based on their 10000 × Ga/Al ratios (Whalen *et al*., 1987), all the alkaline granite samples fall in the A-type granite field (Fig. 7).

The alkaline granites (except sample HY6) have high total rare earth element (REE) abundances, up to 343.5 ppm for sample HY5. The chondrite-normalized REE patterns show slight enrichment in light REE (LREE) with $(La/Yb)_N$ ratios of 1.23–4.72. Both the LREE and heavy REE (HREE) part of the patterns are flat with $(La/Sm)_N$ = 1.33–2.66 and $(Gd/Yb)_N$ = 0.95–1.66. It is worth noting that all the samples have very large negative Eu anomalies (Eu/Eu* = 0.01–0.07), and hence the REE patterns are typical V-shaped (Fig. 8).

Nd isotopes

Table 4 presents the results of Sm–Nd isotopic analyses for three alkaline granites from Huangyangshan de-

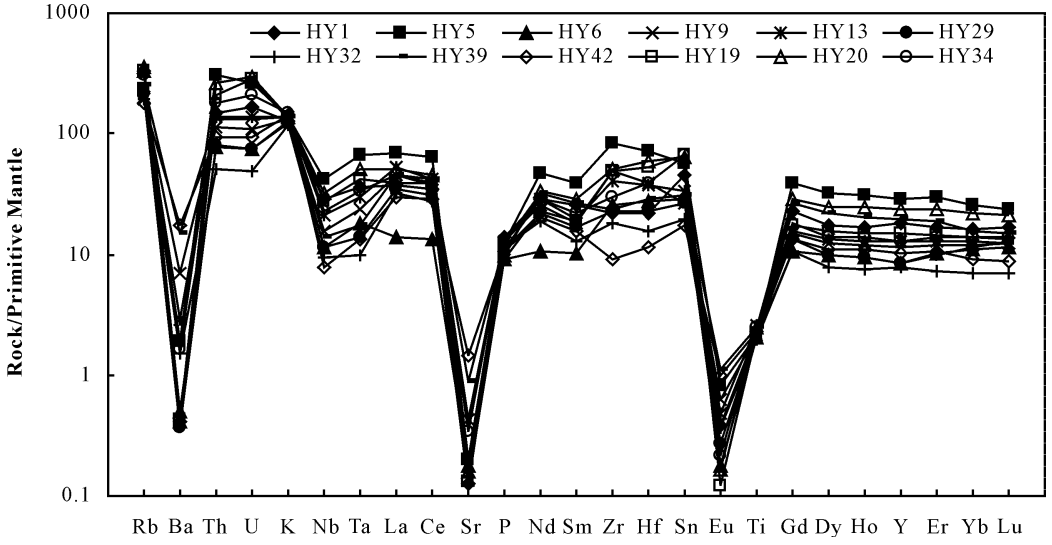

Fig. 6. Primitive-mantle (PM) normalized spidergrams for the alkaline granites from East Junggar. Elements are arranged in the order of decreasing incompatibility from left to right. The PM values are from Sun and McDonough (1989).

termined here and three samples of aluminous A-type, biotite granites from Sujiquan reported previously by Su *et al*. (2006). The initial Nd isotopic compositions are calculated using an age of 305 Ma. As shown in Table 4, all the alkaline granites possess high positive $\varepsilon_{Nd}(T)$ values between +5.9 and +6.5 and relatively young two-stage Nd model ages (T_{DM2}), ranging from 538 to 587 Ma.

Based on their Nd isotopic compositions, the late Carboniferous (*ca*. 305 Ma) alkaline granites of the Karamaili tectonic belt of eastern Junggar were probably derived by partial melting of either: (1) juvenile crust that had formed during the Eocambrian; or (2) a mixture of depleted mantle and ancient (Precambrian) crust.

DISCUSSION

Petrogenesis of the alkaline granites

Turner *et al*. (1992) and Han *et al*. (1997) suggested that A-type granites with high positive $\varepsilon_{Nd}(T)$ and low I_{Sr} values from South Australia and North Xinjiang were generated by extensive fractional crystallization from mantle-derived mafic magmas. Nd isotopic results determined here show that the alkaline granites in the Karamaili tectonic belt have $\varepsilon_{Nd}(T)$ values ranging from +5.9 to +6.5, which are much higher than those for A-type granites from South Australia, with $\varepsilon_{Nd}(T)$ values of +2 to –3 (Turner *et al*., 1992). This could be interpreted to indicate that the alkaline granites in this study were also from extreme fractionation from mantle-derived, mafic magmas. However, the following points are not in favor of this model:

(1) Large volumes of gabbroic and dioritic rocks might be expected to be cropping out around the alkaline gran-

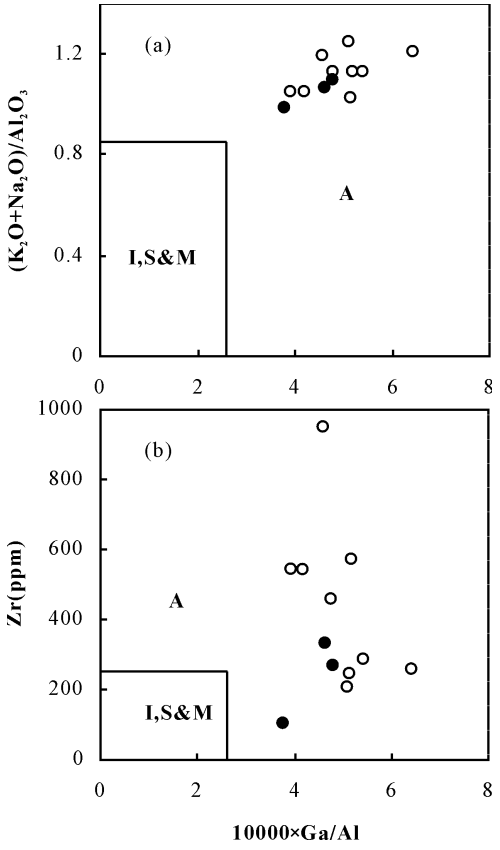

Fig. 7. $(K_2O + Na_2O)/Al_2O_3$ and Zr vs. 10000 × Ga/Al discrimination diagrams of Whalen et al. (1987), showing the A-type nature of the alkaline granites from East Junggar. The symbols are the same as those in Fig. 5.

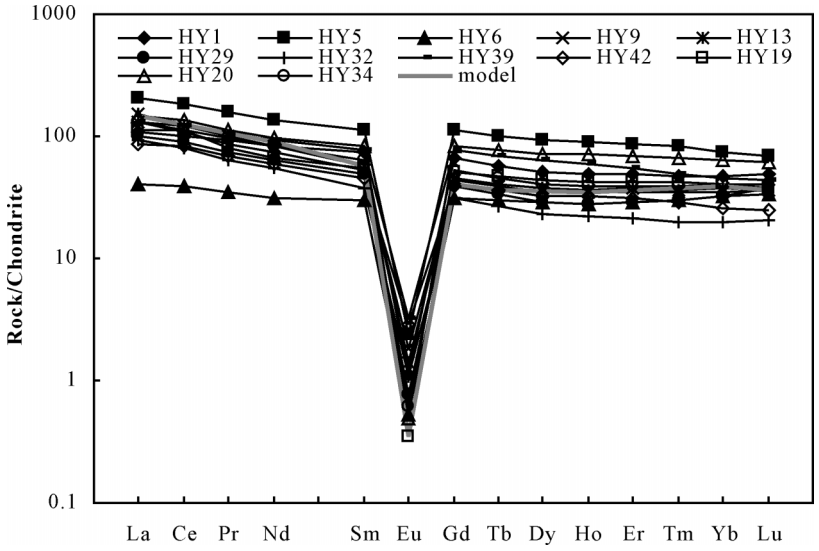

Fig. 8. Chondrite-normalized REE patterns for the alkaline granites from East Junggar. The gray line without marks represents the composition of the model as predicted by REE modeling. The chondrite values for the normalization are from Sun and McDonough (1989).

Table 4. Nd isotopic data for granitoids from East Junggar

Sample	Sm (ppm)	Nd (ppm)	$^{147}Sm/^{144}Nd$	$^{143}Nd/^{144}Nd$	$2\sigma_m$	$\varepsilon_{Nd}(T)$	T_{DM} (Ma)	T_{DM2} (Ma)	$f_{Sm/Nd}$
HY9	8.42	36.46	0.1396	0.512853	6	6.4	612	545	–0.29
HY13	9.13	41.64	0.1326	0.512843	4	6.5	578	538	–0.33
HY42	6.62	26.51	0.1510	0.512849	6	5.9	732	587	–0.23
SJ15	10.44	39.87	0.1583	0.512884	5	6.3	732	555	–0.20
SJ37	10.19	34.40	0.1765	0.512905	5	6.0	1004	579	–0.10
SJ39	7.66	38.95	0.1189	0.512785	5	5.9	588	587	–0.40

Note: $T_{DM} = 1/\lambda \times In[1 + ((^{143}Nd/^{144}Nd)_{sample} - (^{143}Nd/^{144}Nd)_{DM})/((^{147}Sm/^{144}Nd)_{sample} - (^{147}Sm/^{144}Nd)_{DM})]$, T_{DM2} represents two-stage model age, defined as: $T_{DM2} = 1/\lambda \times In\{1 + [(^{143}Nd/^{144}Nd)_{sample} - ((^{147}Sm/^{144}Nd)_{sample} - (^{147}Sm/^{144}Nd)_{cc}) \times (e^{\lambda t} - 1)(^{143}Nd/^{144}Nd)_{DM}]/((^{147}Sm/^{144}Nd)_{cc} - (^{147}Sm/^{144}Nd)_{DM})\}$, among which, $(^{147}Sm/^{144}Nd)_{cc} = 0.1180$, $(^{147}Sm/^{144}Nd)_{DM} = 0.2136$, $(^{143}Nd/^{144}Nd)_{DM} = 0.513151$, and t = the emplacement age of the granite.

Three samples (SJ15, SJ37 and SJ39) are biotite granites from Sujiquan, their isotopic results are from Su et al. (2006).

ites if extensive fractional crystallization took place, but these rocks are rarely found. In fact, many geologists have noted previously that mafic-intermediate rocks which are spatially and temporally associated with A-type granites are usually rare to absent, and so they have argued against the extensive differentiation model (Sylvester, 1989; Wu *et al*., 2002);

(2) As silicate minerals such as hornblende and clinopyroxene have low partition coefficients for Nb and the fractionation of these minerals have little influence on Nb/Ta ratios (Green, 1995), the differentiates of basic magmas are likely to have little or no negative Nb anomalies in the spidergrams (Han *et al*., 1997), but this is not the case for the alkaline granites here. Fractionation of titanate minerals with high partition coefficients for Nb can result in the Nb depletion, but this will increase Nb/Ta ratios in residual magmas simultaneously (Green, 1995), which is not observed for the alkaline granites in this study;

(3) Discrimination diagrams of Pearce (1996) and Eby (1992) reveal that the alkaline granites are similar to post-collision granites of other terranes (Fig. 9a), and more specifically fall into the A2 subgroup (Fig. 9b). Eby (1992) proposed that the A2 subgroup represents magmas derived from continental crust or underplated crust that has been through a cycle of continent-continent collision or island-arc magmatism, mainly because this subgroup is characterized by ratios that vary from those observed for continental crust to those observed for island-arc basalts. This is not consistent with an origin of the granites by fractionation of mantle-derived magmas;

(4) The alkaline granites of eastern Junggar show a

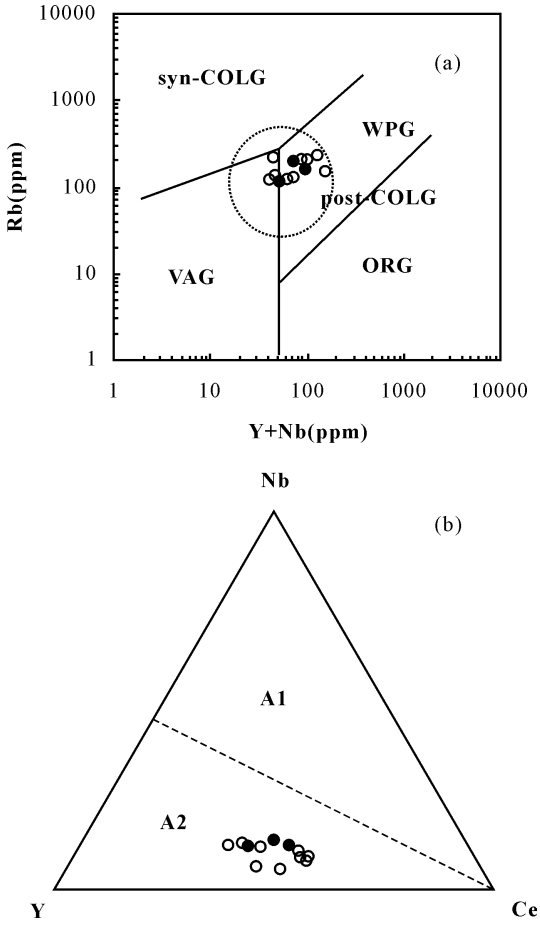

Fig. 9. (a) Rb vs. Y + Nb tectonic discriminant diagram of Pearce (1996). ORG-Ocean Ridge Granites, VAG-Volcanic Arc Granites, syn-COLG-syn-collision Granites, post-COLG-post-collision Granites, WPG-Within Plate Granites; (b) Nb–Y–Ce discriminant diagram for the subdivision of A-type granites (after Eby, 1992). Same symbols as Fig. 5.

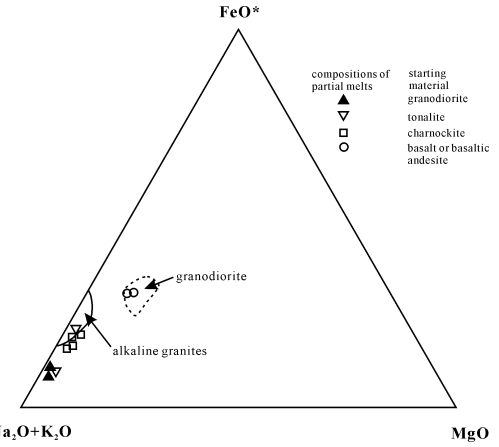

Fig. 10. AFM (wt %) plot of the alkaline granites and granodiorites in this study. The field bounded by solid line represents the range of composition observed for the alkaline granites, and that defined by the dashed line are for the granodiorites of northern of Beilekuduke pluton. Chemical compositions of granodiorites are from H-f, Tang (unpublished data). Experimental products derived from a variety of crustal rocks by water-undersaturated melting are shown for comparison. Experimental data for granodiorite and tonalite, charnockite, basalt and basaltic andesite are from Patiño Douce (1997), Beard et al. (1994), Beard and Lofgren (1991) respectively.

relatively large variation of T_{DM} because of the variation of $f_{Sm/Nd}$; however, their two-stage model ages (T_{DM2}) are some 250 Ma older than their crystallization ages and fall within a narrow range. Consequently, the alkaline granites were not derived directly from a depleted mantle, but instead most likely interacted with crustal sources.

Clemens *et al.* (1986) and Collins *et al.* (1982) suggested that A-type granites resulted from partial melting of granulitic residue from which a I-type granitic melt had been previously extracted; this residual model could explain why A-type magmas would contain less amounts of H_2O and occur later in the magmatic history of a terrane than S- or I-type magmas. However, more experimental studies indicated that a residual source will be enriched in Ca, Al and Mg and depleted in K, Si and incompatible elements relative to the original protolith (Creaser *et al.*, 1991), and such a residue is unlikely to generate A-type melts with high SiO_2 and alkalis contents. Furthermore, A-type granites can contain water up to 4.5–6.5% (Dall'Agnol *et al.*, 1999). King *et al.* (1997) showed that aluminous A-type granites in the Lachlan Fold Belt had similar H_2O contents to those of I-type granites. It seems increasingly obvious that crustal rocks that have not undergone any previous partial melting event can be involved in the generation of A-type granites.

Some researchers have noted that dehydration melting of I-type tonalitic or granodioritic rocks in the shallow crust may result in the generation of magmas with A-type affinity (Creaser *et al.*, 1991; Patiño Douce, 1997), but this model cannot explain the geological and geochemical characteristics of the peralkaline A-type granites in this study, because: (1) Partial melts of granodioritic rocks do not have the same major element compositions as peralkaline A-type granites; for example, the former are more enriched in alkalis and depleted in FeO* (Fig. 10); (2) Alkaline granites and I-type granodiorites of eastern Junggar were generated at similar times and emplaced at similar tectonic setting; thus, the I-type granodiorites cannot represent an A-type source for partial melting in this particular region. The possibility of direct partial melting of a more ancient (pre-Eocambrian) I-type granitic source is unlikely based on the high $\varepsilon_{Nd}(T)$ values of the alkaline granites.

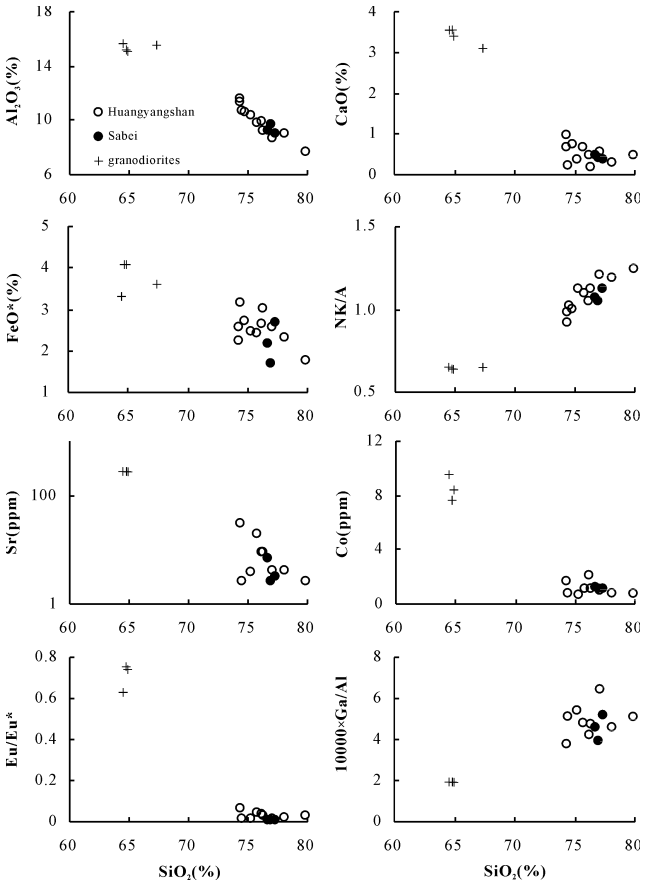

Fig. 11. Plots of SiO_2 vs. other oxides, elements and ratios for granitoids from East Junggar.

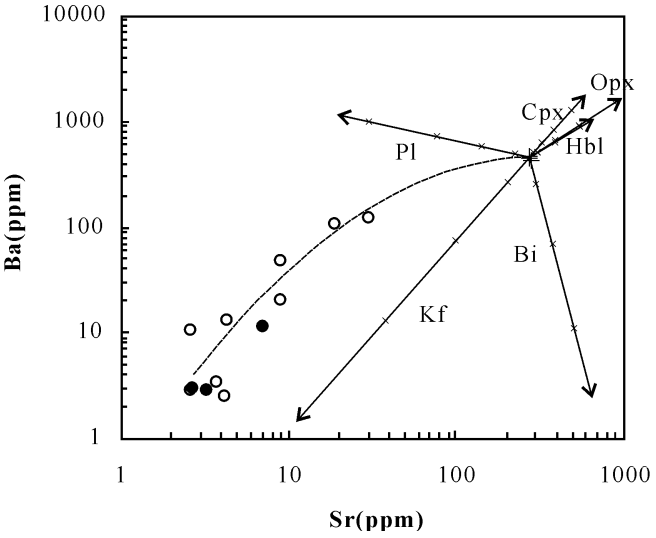

Fig. 12. Ba vs. Sr diagram for granitoids from East Junggar. The least evolved granodiorites are taken as the parental magma compositions. Fractionation trends are calculated for Rayleigh fractionation of clinopyroxene (Cpx), orthopyroxene (Opx), hornblende (Hbl), plagioclase (Pl), biotite (Bi), and K-feldspar (Kf). Tick marks represent 10%, 30%, 50%, 70% fractional crystallization from the melt. The trend of the line shows the compositional change in the residual liquid when the specified phase is progressively removed from the magma during fractional crystallization. The symbols are the same as in Fig. 11.

More recently, Rajesh (2000) and Frost *et al*. (2002) pointed out that A-type granites are often associated in space and time with anorthosite and charnockite complexes, with which they may have had a close genetic relationship. For example, A-type granites may be generated by partial melting of lower crustal charnockitic rocks or by differentiation of ferrodioritic magmas residual to anorthosite. These models can be ruled out in eastern Junggar because such source rocks have not been found in the Karamaili tectonic belt although partial melting of charnockite could explain the major element characteristics of the peralkaline A-type granites (Fig. 10).

From above discussion, we consider that the alkaline granites of eastern Junggar may have been formed by fractional crystallization of the parent magmas of the I-type granodioritic rocks of the region. Partial melting process alone cannot be used to explain the geochemical characteristics of the alkaline granites. The granodioritic rocks associated with the alkaline granites have high Ba and Sr concentrations and negligible negative Eu anomalies (unpublished data). Moreover, they possess $\varepsilon_{Nd}(T)$ values of about +6.1 (unpublished data), which are identical to those of the alkaline granites. Hence they can be regarded as the parental magmas for the alkaline granites.

From the granodiorites to the alkaline granites, with increasing SiO_2 content, concentrations of major elements (such as Al_2O_3, CaO, FeO*) and trace elements (such as Sr, Co) and some ratios (such as NK/A, 10000 × Ga/Al) show regular linear variation trends (Fig. 11), consistent with a comagmatic relationship between these temporally and spatially associated rocks. There are apparent gaps in the silica range between the granodiorites and alkaline granites in Fig. 11 but this may simply be because sampling of granodioritic rocks has been restricted to only small areas.

FeO*, MgO, Co, and Cr contents all decrease significantly with increasing SiO_2, which is interpreted as the result of fractionation of ferromagnesian phases such as biotite and hornblende. The strong depletions in Ba, Sr and Eu as shown in the spidergrams and REE patterns may result from the fractional crystallization of plagioclase and potassium feldspar during magma evolution. In addition, the Ba vs. Sr relationships shown in Fig. 12 suggest that the fractionation of plagioclase and potassium feldspar both played a major role in earlier differentiation stages, but that potassium feldspar separation dominated in later stages. Therefore, the alkaline

Table 5. Results of trace element modeling

	Concentration in parent (C_0)	Bulk distribution coefficient (D)	Calculated concentration (C_l)	Actual concentration (HY13)
Ba	459	3.244	20.4	20.5
Sr	275	3.468	8.98	8.99
Y	24.8	0.390	57.7	58.0
La	17.5	0.516	34.3	36.1
Nd	18.8	0.438	41.1	39.2
Sm	3.82	0.403	8.74	8.76
Eu	0.78	3.633	0.02	0.08
Gd	3.77	0.435	8.25	9.29
Tb	0.63	0.458	1.33	1.52
Ho	0.88	0.424	1.96	2.07
Yb	3.39	0.528	6.52	6.28
Lu	0.49	0.549	0.91	0.92

Note: Fractionating minerals involve plagioclase (43%), K-feldspar (40.5%), hornblende (6%), biotite (6.5%), quartz (4%), allanite (0.03%) and zircon (0.03%). The composition of parental magmas is from H-f, Tang (unpublished data).

granites could have been generated by differentiation of the granodioritic melts via removal of plagioclase, potassium feldspar, biotite, and hornblende.

Previous studies (Clemens *et al*., 1986; Turner *et al*., 1992; Landenberger and Collins, 1996) show that both alkalis and fluorine contents increase in residual granitic magmas with fractionation. HFSE such as zirconium in alkali-fluorine rich magmas will form alkali-fluoro-complexes, leading to precipitation of zircon and the enrichment of alkalis and fluorine in the evolved magmas. Malvin and Drake (1987) noted that plagioclase fractionation can account for depletion of Sr and Ba and high $10000 \times Ga/Al$ ratios in residual magmas that could have formed A-type granites.

In order to illustrate a plausible fractional crystallization origin for the alkaline granites, the equation for Rayleigh fractional crystallization was used:

$$C_1 = C_0 f^{(D-1)}$$

in which C_1 is the concentration of an element in the residual liquid, C_0 is the concentration of an element in the original parent magma, f is the fraction of remaining melt and D is the bulk distribution coefficient for the element. For the model, a granodioritic rock from eastern Junggar (H-f, Tang, unpublished data) and sample HY13 of this study were used to represent the original parent magma and residual liquid respectively. The proportion of the fractionating mineral assemblage was 43% plagioclase, 40.5% K-feldspar, 6% hornblende, 6.5% biotite, 4% quartz, 0.03% allanite and 0.03% zircon, and the fraction of remaining melt was 25% ($f = 0.25$). These assumed parameters may be valid, the evidences include: (1) High SiO_2 contents of the alkaline granites reveal a much greater degree of fractionation; (2) The geochemical properties show that fractionation is dominated by removal of both plagioclase and potassium feldspar, with minor involvement of hornblende and biotite (see the above discussion); (3) Allanite should be included in the calculation to reduce LREE contents of residual melt, zircon should also be used to explain the observed REE patterns of the alkaline granites. With these parameters, model compositions were calculated using literature values for partition coefficients for dacites and rhyolites. The results show that the calculated composition of the residual magma agrees well with observed compositions of the alkaline granites (Table 5), including the REE patterns (Fig. 8). The main implication of the model is that granodioritic magmas would have had to have undergone high degrees of fractional crystallization (75%) in order to produce residual magmas with compositions like those of the alkaline granites.

The granodioritic rocks of eastern Junggar were most likely produced by partial melting of lower crustal basaltic to andesitic rocks. Figure 10 shows that partial melts of basalt and basaltic andesite sources at 900–1000°C (Beard and Lofgren, 1991) fall within the field of the granodioritic rocks. Experimental investigations conducted by Rapp and Watson (1995) also demonstrated that intermediate to silicic melts could be produced by dehydration melting of basaltic rocks. Combined with the high $\varepsilon_{Nd}(T)$ values of the granodiorites and alkaline granites, consistent with their derivation from Eocambrian crustal rocks, source rocks may have been deeply buried into the lower crust during late Paleozoic subduction and accretion (Chen and Jahn, 2004; Chen and Arakawa, 2005). This perspective is supported by the evidence that partial melting of basic oceanic crustal materials can yield highly siliceous acidic magmas (Peacock *et al*., 1994). Moreover, Kwon *et al*. (1989) argued that aluminous A-type granites from West Junggar, Xinjiang, were derived from source materials with an oceanic affinity.

Relationship between the alkaline granites and mineralization

Tin mineralization is commonly related to fractionated, ilmenite-bearing S-type granites. These evolved peraluminous granites are thought to be the chief source of tin mineralization. They typically contain muscovite, garnet, topaz, and tourmaline, and possess low $\varepsilon_{Nd}(T)$ values (<0) and high initial $^{87}Sr/^{86}Sr$ ratios (Linnen, 1998; Yokart *et al*., 2003; Esmaeily *et al*., 2005). In contrast, the alkaline granites of this study are peralkaline with an A-type affinity, and have high $\varepsilon_{Nd}(T)$ values between +5.9 and +6.5: they are quite different from "typical" stanniferous granites with S-type affinities. Thus, the relationship between the alkaline granites and tin mineralization in the Karamaili tectonic belt is potentially of great significance.

Although the Re–Os system may be disturbed by secondary hydrothermal alteration and give erroneous ages (McCandless *et al*., 1993; Suzuki *et al*., 2000), our molybdenite samples were collected from one tunnel with short sampling intervals, and petrographic observations show that all the molybdenite are well-formed and form euhedral grains with no inclusions. In addition, model ages for six individual analyses cluster in a narrow range, and within error all fall along a single ^{187}Os–^{187}Re isochron. The sum of the evidence is that the Re–Os results reflect the mineralization age and not a later alteration event. Therefore, the mineralization age for the Sareshike tin deposit is consistent with the intrusive age of the alkaline granites (both are about 305 Ma). Considering both the similar age and spatial relationship between the tin deposit and the alkaline granites, we conclude that there is a close genetic connection between them.

Mao *et al*. (1999) and Stein *et al*. (2001) have summarized how the Re content in molybdenite may reflect the source of the ore-forming fluids. Stein *et al*. (2001) suggested that deposits with a mantle component in their sources have significantly higher Re contents than those deposits that are crustally derived. By comparison with published Re contents of molybdenite from well-studied molybdenite-bearing deposits worldwide, Mao *et al*. (1999) concluded that Re abundances in molybdenite commonly decrease from mantle sources, to mixtures between mantle and crustal sources, and to crustal sources. The Re contents in our molybdenite are very low, with range of 0.323 to 0.961 ppm, suggesting that the ore-forming fluids that formed them had a crustal affinity.

Stein (2006) recently argued that low Re concentrations in molybdenite (<20 ppm and commonly at the sub-ppm level) were a strong evidence of a metamorphic derivation, and that related deposits had sub-economic potential. In the Karamaili tectonic belt, however, almost no metamorphism has occurred in the studied area since the late Carboniferous, tin deposits in the area are presently being mined and the belt is prospective for other economic deposits. Consequently, we argue that the low Re concentrations in the studied molybdenite are indicative of a crustal source, but not of a metamorphic origin.

Liu *et al*. (1996) found that fluid inclusions hosted within quartz from the Sareshike cassiterite-quartz veins had compositional features similar to those of the alkaline granites. Also, oxygen and hydrogen isotopic compositions of quartz in the veins suggest that the ore-forming hydrothermal fluids in equilibrium with quartz had magmatic water sources. These data are compatible with the ore-forming fluids being derived from the late-stage differentiation of the alkaline granitic magmas, and hence the tin deposits being of magmatic hydrothermal type.

In West Junggar, several gold deposits are closely related to the aluminous A-type granites along the Darabut tectonic belt (Li *et al*., 2000). Compared to the alkaline granites in this study, the granitoids in West Junggar studied by Chen and Arakawa (2005) are less evolved with higher Ba, Sr contents and Eu/Eu* ratios and lower SiO_2, Rb, Sn contents, which may be the reason for the lack of Sn mineralization in West Junggar. Although like the tin deposits, the known gold deposits are small to medium in size, they are important because they provide a good opportunity to study the relationship between A-type granites and metal mineralization. They also have significance for developing exploration strategies for mineral resources associated with A-type granites in Northern Xinjiang and in other areas.

Conclusions

(1) The alkaline granites from the Karamaili tectonic belt possess characteristics of typical peralkaline A-type granites: they contain alkalic mafic minerals such as riebeckite and aegirine, and have high contents of alkalis but low abundances of Al_2O_3, CaO, MgO, FeO*. They show flat V-shaped REE patterns, and are characterized by significant enrichment of some LILE, HFSE, and strong depletion in Ba, Sr, Eu, and to a lesser extent, Nb.

(2) Weighted mean $^{206}Pb/^{238}U$ ages for three alkaline granites were obtained by LA-ICPMS measurements: two from Huangyangshan are 302 ± 2 Ma and 310 ± 4 Ma, and the third one from Sabei is 306 ± 3 Ma. These data show that the age of the alkaline granites is about 305 Ma. Six molybdenite samples from the Sareshike tin deposit, associated with the alkaline granites, yielded an ^{187}Os–^{187}Re isochron age of 307 ± 11 Ma and weighted mean model age of 306.5 ± 3.4 Ma. The geochronology results suggest that both the alkaline granites and tin deposits formed in the late Carboniferous and may be genetically related.

(3) The late Carboniferous alkaline granites possess

high positive $\varepsilon_{Nd}(T)$ values between +5.9 and +6.5 and two-stage Nd model ages (T_{DM2}) ranging from 538 to 587 Ma. They were most likely formed by fractional crystallization of parental granodioritic magmas associated them. The granodiorites were most likely produced by partial melting of basaltic oceanic crustal rocks deeply buried into lower crust during late Paleozoic subduction and accretion.

(4) The Re–Os isotopic ages for the molybdenite samples reflect their mineralization age and not a later alteration event. Furthermore, the low Re contents (0.323–0.961 ppm) of the molybdenite deposits suggest a crustal source, most probably related to the alkaline granites with which they are associated. Economic tin deposits may not be genetically related only to peraluminous S-type granites, but also to peralkaline A-type granites.

Acknowledgments—We are very grateful to Mr. Mike Tubrett and Dr. Marc Poujol at MUN for their technical assistance with the U–Pb and Nd isotope analyses. Constructive reviews by R. A. Creaser and an anonymous reviewer have substantially improved the manuscript. This work was supported by the Natural Science Foundation of China (Grant No. 40772044).

REFERENCES

Beard, J. S. and Lofgren, G. E. (1991) Dehydration melting and water-saturated melting of basaltic and andesitic greenstones and amphibolites at 1, 3, and 6.9 kb. *J. Petrol.* **32**, 365–401.

Beard, J. S., Lofgren, G. E., Sinha, A. K. and Tollo, R. P. (1994) Partial melting of apatite-bearing charnockite, granulite, and diorite: melt compositions, restite mineralogy, and petrologic implications. *J. Geophys. Res.* **99**, 591–603.

Bi, C. S., Shen, X. Y., Xu, Q. S., Ming, K. H., Sun, H. L. and Zhang, C. S. (1993) Geological characteristics of stanniferous granites in the Beilekuduk tin metallogenic belt, Xinjiang. *Acta Petrol. Mineral.* **12**, 213–223 (in Chinese with English abstract).

Chappell, B. W. and White, A. J. R. (1974) Two contrasting granite types. *Pacific Geol.* **8**, 173–174.

Chen, B. and Arakawa, Y. (2005) Elemental and Nd–Sr isotopic geochemistry of granitoids from the West Junggar foldbelt (NW China), with implications for Phanerozoic continental growth. *Geochim. Cosmochim. Acta* **69**, 1307–1320.

Chen, B. and Jahn, B. M. (2004) Genesis of post-collisional granitoids and basement nature of the Junggar Terrane, NW China: Nd–Sr isotope and trace element evidence. *J. Asian Earth Sci.* **23**, 691–703.

Chen, F. W., Li, H. Q., Cai, H., Liu, Q. and Chang, H. L. (1999) Chronology and origin of the Gangliangzi tin orefield, Xinjang. *Mineral Deposits* **18**, 91–97 (in Chinese with English abstract).

Clemens, J. D., Holloway, J. R. and White, A. J. R. (1986) Origin of an A-type granite: Experimental constraints. *Am. Mineral.* **71**, 317–324.

Collins, W. J., Beams, S. D., White, A. J. R. and Chappell, B. W. (1982) Nature and Origin of A-type Granites with Particular Reference to Southeastern Australia. *Contrib. Mineral. Petrol.* **80**, 189–200.

Creaser, R. A., Price, R. C. and Wormald, R. J. (1991) A-type granites revisited: Assessment of a residual-source modal. *Geology* **19**, 163–166.

Dall'Agnol, R., Scaillet, B. and Pichavant, M. (1999) An experimental study of a lower Proterozoic A-type granite from the eastern Amazonian cration, Brazil. *J. Petrol.* **40**, 1673–1698.

Du, A. D., He, H. L., Yin, N. W., Zou, X. Q., Sun, Y. L., Sun, D. Z., Chen, S. Z. and Qu, W. J. (1994) A study on the rhenium—osmium geochronometry of molybdenites. *Acta Geologica Sinica* **68**, 339–347 (in Chinese with English abstract).

Eby, G. N. (1990) The A-type granitoids: A review of their occurrence and chemical characteristics and speculations on their petrogenesis. *Lithos* **26**, 115–134.

Eby, G. N. (1992) Chemical subdivision of the A-type granitoids: Petrogenetic and tectonic implications. *Geology* **20**, 641–644.

Esmaeily, D., Nédélec, A., Valizadeh, M. V., Moore, F. and Cotten, J. (2005) Petrology of the Jurassic Shah-Kuh granite (eastern Iran), with reference to tin mineralization. *J. Asian Earth Sci.* **25**, 961–980.

Frost, B. R., Barnes, C. G., Collins, W. J., Arculus, R. J., Ellis, D. J. and Frost, C. D. (2001) A geochemical classification for granitic rocks. *J. Petrol.* **42**, 2033–2048.

Frost, C. D., Frost, B. R., Bell, J. M. and Chamberlain, K. R. (2002) The relationship between A-type granites and residual magmas from anorthosite: evidence from the northern Sherman batholith, Laramie Mountains, Wyoming, USA. *Precambrian Res.* **119**, 45–71.

Green, T. H. (1995) Significance of Nb/Ta as an indicator of geochemical processes in the crust-mantle system. *Chem. Geol.* **120**, 347–359.

Han, B. F., Wang, S. G., Jahn, B. M., Hong, D. W., Kagami, H. and Sun, Y. L. (1997) Depleted-mantle source for the Ulungur River A-type granites from North Xinjiang, China: geochemistry and Nd–Sr isotopic evidence, and implications for Phanerozoic crustal growth. *Chem. Geol.* **138**, 135–159.

Hou, Z. Q., Qu, X. M., Wang, S. X., Du, A. D., Gao, Y. F. and Huang, W. (2004) Re–Os age for molybdenite from the Gangdese porphyry copper belt on Tibetan plateau: implication for geodynamic setting and duration of the Cu mineralization. *Science in China: Series D* **147**, 221–231.

Jackson, S. E., Longerich, H. P., Horn, I. and Dunning, G. R. (1996) The application of laser ablation micrcoprobe (LAM)-ICP-MS to *in situ* U–Pb zircon geochronology. *J. Conf. Abstract*, **1**, 283.

Kerr, A. and Fryer, B. J. (1993) Nd isotope evidence for crust-mantle interaction in the generation of A-type granitoid suites in Labrador, Canada. *Chem. Geol.* **104**, 39–60.

King, P. L., White, A. J. R., Chappell, B. W. and Allen, C. M. (1997) Characterization and origin of aluminous A-type granites from the Lachlan fold belt, Southeastern Australia. *J. Petrol.* **38**, 371–391.

Klimn, K., Holtz, F., Johannes, W. and King, P. L. (2003) Fractionation of metaluminous A-type granites: an experimental study of the Wangrah Suite, Lachlan Fold Belt, Australia. *Precambrian Res*. **124**, 327–341.

Kwon, S. T., Tilton, G. R., Coleman, R. G. and Feng, Y. (1989) Isotopic studies bearing on the tectonics of the West Junggar region, Xinjiang, China. *Tectonics* **8**, 719–727.

Landenberger, B. and Collins, W. J. (1996) Derivation of A-type granites from a dehydrated charnockitic lower crust: Evidence from the Chaelundi Complex, eastern Australia. *J. Petrol*. **37**, 145–170.

Li, H. Q., Chen, F. W. and Cai, H. (2000) Study on Rb–Sr isotopic ages of gold deposits in West Junggar area, Xinjiang. *Acta Geologica Sinica* **74**, 181–192 (in Chinese with English abstract).

Li, J. Y. (1995) Main characteristics and emplacement processes of the east Junggar ophiolites, Xinjiang, China. *Acta Petrologica Sinica* **11** (Suppl.), 73–84 (in Chinese with English abstract).

Li, J. Y., Xiao, X. C., Tang, Y. Q., Zhao, M., Zhu, B. Q. and Feng, Y. M. (1990) Main characteristics of late paleozoic plate tectonics in the southern part of east Junggar, Xinjiang. *Geol. Rev*. **36**, 305–316 (in Chinese with English abstract).

Linnen, R. L. (1998) Depth of emplacement, fluid provenance and metallogeny in granitic terranes: a comparison of western Thailand with other tin belts. *Mineralium Deposita* **33**, 461–476.

Liu, J. Y., Yuan, K. R., Wu, G. Q., Xin, J. G. and Liu, S. (1996) *A Study on Alkali-Rich Granitoids and Related Mineralization in Eastern Junggar, Xinjiang, China*. Central South University of Technology Press, Changsha (in Chinese with English abstract).

Liu, J. Y., Yu, H. X. and Wu, G. Q. (1997) Alkali granites and tin deposits of the Kalamali area, northern Xinjiang. *Geological Exploration for Non-Ferrous Metals* **6**, 129–135 (in Chinese with English abstract).

Loiselle, M. C. and Wones, D. R. (1979) Characteristics and origin of anorogenic granites (abstract). *Geol. Soc. Am*. **11**, 468.

Ludwig, K. R. (1999) Isoplot/Ex v. 2.6. Berkeley Geochronological Center Spec. Publ., No. 1a.

Malvin, D. J. and Drake, M. J. (1987) Experimental determination of crystal/melt partitioning of Ga and Ge in the system forsterite-anorthite-diopside. *Geochim. Cosmochim. Acta* **51**, 2117–2128.

Mao, J. W., Zhang, Z. C., Zhang, Z. H. and Du, A. D. (1999) Re–Os isotopic dating of molybdenites in the Xiaoliugou W (Mo) deposit in the northern Qilian mountains and its geological significance. *Geochim. Cosmochim. Acta* **63**, 1815–1818.

Mao, J. W., Du, A. D., Seltmann, R. and Yu, J. J. (2003). Re–Os ages for the Shameika porphyry Mo deposit and the Lipovy Log rare metal pegmatite, central Urals, Russia. *Mineralium Deposita* **38**, 251–257.

Markey, R., Stein, H. and Morgan, J. (1998). Highly precise Re–Os dating for molybdenite using alkaline fusion and NTIMS. *Talanta* **45**, 935–946.

McCandless, T. E., Ruiz, J. and Campbell, A. R. (1993) Rhenium behavior in molybdenite in hypogene and near-surface environments: implications for Re–Os geochronology. *Geochim. Cosmochim. Acta* **57**, 889–905.

Nardi, L. V. S. and Bonin, B. (1991) Post-orogenic and non-orogenic alkaline granite associations: the Saibro intrusive suite, southern Brazil—A case study. *Chem. Geol*. **92**, 197–211.

Patiño Douce, A. E. (1997) Generation of metaluminous A-type granites by low-pressure melting of calc-alkaline granitoids. *Geology* **25**, 743–746.

Peacock, S. M., Rushmer, T. and Thompson, A. B. (1994) Partial melting of subducting oceanic crust. *Earth Planet. Sci. Lett*. **121**, 227–244.

Pearce, J. A. (1996) Sources and settings of granitic rocks. *Episodes* **19**, 120–125.

Qu, W. J. and Du, A. D. (2003) Highly precise Re–Os dating of molybdenite by ICP-MS with Carius tube sample digestion. *Rock and Mineral Analysis* **22**, 254–257 (in Chinese with English abstract).

Rajesh, H. M. (2000) Characterization and origin of a compositionally zoned aluminous A-type granite from South India. *Geol. Mag*. **137**, 291–318.

Rapp, R. P. and Watson, E. B. (1995) Dehydration melting of metabasalt at 8–32 kbar: implications for continental growth and crust-mantle recycling. *J. Petrol*. **36**, 891–931.

Shirey, S. B. and Walker, R. J. (1995) Carius tube digestion for low-blank rhenium-osmium analysis. *Anal. Chem*. **67**, 2136–2141.

Shu, L. S. and Wang, Y. J. (2003) Late Devonian–early Carboniferous radiolarian fossils from siliceous rocks of the Kelameili ophiolite, Xinjiang. *Geol. Rev*. **49**, 408–413 (in Chinese with English abstract).

Sláma, J., Košler, J., Crowley, J. L., Gerdes, A., Horstwood, M. S. A., Morris, G. A., Nasdala, L., Norberg, N., Schaltegger, U., Tubrett, M. N. and Whitehouse, M. J. (in review) Plešovice zircon—a new natural standard for U–Pb and Hf isotopic microanalysis. *Chem Geol*.

Stein, H. J. (2006) Low-rhenium molybdenite by metamorphism in northern Sweden: Recognition, genesis, and global implications. *Lithos* **87**, 300–327.

Stein, H. J., Markey, R. J., Morgan, J. W., Du, A. and Sun, Y. (1997) Highly precise and accurate Re–Os ages for molybdenite from the East Qinling molybdenum belt, Shaanxi Province, China. *Econ. Geol*. **92**, 827–835.

Stein, H. J., Markey, R. J., Morgan, J. W., Hannah, J. L. and Schersten, A. (2001) The remarkable Re–Os chronometer in molybdenite: how and why it works. *Terra Nova* **13**, 479–486.

Su, Y. P., Tang, H. F., Liu, C. Q., Hou, G. S. and Liang, L. L. (2006) The determination and a preliminary study of Sujiquan aluminous A-type granites in East Junggar, Xinjiang. *Acta Petrol. Mineral*. **25**, 175–184 (in Chinese with English abstract).

Sun, S. S. and McDonough, W. F. (1989) Chemical and isotopic systematics of oceanic basalts: implications for mantle composition and processes. *Magmatism in the Ocean Basins* (Saunders, A. D. and Norry, M. J., eds.), **42**, 313–345, Geol. Soc. Spec. Publ.

Suzuki, K., Kagi, H., Nara, M., Takano, B. and Nozaki, Y. (2000) Experimental alteration of molybdenite: evaluation of the

Re–Os system, infrared spectroscopic profile and polytype. *Geochim. Cosmochim. Acta* **64**, 223–232.

Sylvester, P. J. (1989) Post-collisional alkaline granites. *J. Geol.* **97**, 261–280.

Sylvester, P. J. (1994) Archean granite plutons. *Archean Crustal Evolution* (Condie, K. C., ed.), Elsevier, Developments in Precambrian Geology, II, 261–314.

Tang, H. F., Su, Y. P., Liu, C. Q., Hou, G. S. and Wang, Y. B. (2007) Zircon U–Pb age of the plagiogranite in Kalamaili belt, northern Xinjiang and its tectonic implications. *Geotectonica et Metallogenia* **31**, 110–117 (in Chinese with English abstract).

Taylor, R. P., Strong, D. F. and Fryer, B. J. (1981) Volatile control of contrasting trace element distributions in peralkaline granitic and volcanic rocks. *Contrib. Mineral. Petrol.* **77**, 267–271.

Turner, S. P., Foden, J. D. and Morrison, R. S. (1992) Derivation of some A-type magmas by fractionation of basaltic magma: An example from the Padthaway Ridge, South Australia. *Lithos* **28**, 151–179.

Vernikovsky, V. A., Pease, V. L., Vernikovskaya, A. E., Romanov, A. P., Gee, D. G. and Travin, A. V. (2003) First report of early Triassic A-type granite and syenite intrusions from Taimyr: product of the northern Eurasian superplume? *Lithos* **66**, 23–36.

Wang, Z. X., Zhou, G. Z. and Li, T. (2003) The consideration on ophiolite and interrelated issue in northern Xinjiang, northwestern China. *Acta Petrologica Sinica* **19**, 683–691 (in Chinese with English abstract).

Whalen, J. B., Currie, K. L. and Chappell, B. W. (1987) A-type granites: geochemical characteristics, discrimination and petrogenesis. *Contrib. Mineral. Petrol.* **95**, 407–419.

Wu, F. Y., Sun, D. Y., Li, H. M., Jahn, B. M. and Wilde, S. (2002) A-type granites in northeastern China: age and geochemical constraints on their petrogenesis. *Chem. Geol.* **187**, 143–173.

Xin, J. G., Yuan, K. R. and Liu, J. Y. (1995) The alkali granites and their genesis and tectonic significance in the north area of the east Junggar, Xinjiang. *Geotectonica et Metallogenia* **19**, 214–226 (in Chinese with English abstract).

Yokart, B., Barr, S. M., Williams-Jones, A. E. and Macdonald, A. S. (2003) Late-stage alteration and tin-tungsten mineralization in the Khuntan Batholith, northern Thailand. *J. Asian Earth Sci.* **21**, 999–1018.

Yu, H. X., Wu, G. Q. and Liu, J. Y. (1998) The two ore-forming metals series closely related to the two granitoid series in eastern Junggar, Xinjang. *Geotectonica et Metallogenia* **22**, 119–127 (in Chinese with English abstract).